ACEEE Int. J. on Information Technology, Vol. 3, No. 1, March 2013

Graphical User Interface for Benthic Mapping

Hyun Jung Cho[1], Sachidananda Mishra[2], and Deepak R. Mishra[3]
[1] Department of Integrated Environmental Science, Bethune-Cookman University, Daytona Beach, FL 32114, USA
[2]Geo-Systems Research Institute, Mississippi State University, Mississippi State, 39762, USA
[3]Department of Geography, University of Georgia, Athens, GA 30602, USA
Email: [1]choh@cookman.edu,[2]sm1287@msstate.edu, [3]dmishra@uga.edu

***Abstract*—A Graphical User Interface (GUI) was developed for a user-friendly implementation of a water depth correction model. The Interactive Data Language (IDL)-based tool provides the prospective users with an interface that can be applied to perform water depth correction on hyperspectral images that contain shallow water bodies containing benthic habitat information. Users can select a pixel or a subset of a hyperspectral image to be corrected and define water correction for water depths of 0-2.0 m and for turbidity values of 0-20 NTU (Nephalometric Turbidity Unit) using the GUI. The results demonstrate that the GUI is an effective benthic mapping tool for shallow littoral areas; and it can be incorporated as a module in currently available commercial image processing software.**

***Index Terms*— water depth correction, hyperspectral, GUI, benthic habitats**

I. Introduction

Airborne hyperspectral sensors provide data with high spatial and spectral resolutions for advanced remote sensing of the earth surface features. While these hyperspectral data provide detailed information that can be derived from the fine-scaled variations in narrow spectral bands, the compromised radiometric resolutions make the signals prone to scattering and absorption by particles and molecules in the atmosphere. Therefore effective atmospheric correction scheme is used to retrieve above surface remote sensing reflectance (R_{rs}). Several atmospheric correction algorithms have been developed and are available; and some model codes have been successfully imbedded in commercial remote sensing software (i.e. Fast Line-of-sight Atmospheric Analysis of Spectral Hypercubes: FLAASH) [1]. In case of benthic remote sensing, above surface remote sensing reflectance data need to be corrected for the light attenuation in the water column (water column correction) because of absorption and scattering of light by optically active constituents in the water column including water molecules. For remote sensing of ocean and coastal benthic habitats, several radiative transfer or physics based models have been applied to map benthic features including coral reefs and seagrass meadows in relatively clear, deep coastal environments [2], [3], [4], [5], [6]. However, even the commercially available water correction packages, such as HydroLight 5, EcoLight 5 (Sequoia Scientific Inc.), have not been successfully interfaced with mainstream image processing software packages such as ERDAS or ENVI.The purpose of this study is to present a Graphical User Interface (GUI) for a water correction model that can be added as a module in existing image processing software.This model and GUI application are particularly developed and designed for very shallow littoral areas (generally the areas between the shoreline to a water depth of 2 m).

II. Related Work

Success of benthic mapping using space borne/airborne remote sensing depends on the accurate retrieval of the bottom reflectance component from the above surface remote sensing reflectance data. The whole process is even more challenging in coastal and estuarine environments because of the optical complexity due to model spatially and temporally varying water column attenuation in these turbid and often productive waters.

Physics based radiative transfer theory has been used to retrieve bottom reflectance by creating a spectral library of different benthos (bottom substrates and objects) at different water depths and matching the modeled reflectance spectrum from the library with the measured ones [7]. Similarly, [8] developed a hyperspectral remote sensing reflectance model using radiative transfer equations and optimization technique where the model minimizes the error between modeled R_{rs} and the measured R_{rs} spectrum using a predictor-corrector scheme and simultaneously retrieves water column attenuation, depth, and bottom reflectance. However, the major difficulty with this model is its inapplicability in turbid case-2 waters, where the algorithm is likely to perform poorly [9].

Benthic remote sensing research has primarily used spectral band ratio indices to retrieve bathymetry [10]. [11], [12], [5]. Majority of the previous research has used the signal variation in short visible ranges due to their ability to penetrate into the water column [13], [14]; and the Near InfraRed (NIR) wavelengths are often not used due to the high absorption in water [2], [3], [4], [5], [6]. However, bottom backscattering of NIR in the shallow littoral areas can be significant and provide important information, especially in the areas that contain substantial amount of photosynthetic seagrasses, benthic algae, or phytoplankton [15]. In the optically shallow waters, conventional Beer-Lambert's exponential light attenuation of upwelling as well as downwelling light with depth is not applicable because of the high bottom reflectance and wave focusing [3], [12]. Therefore, we previously developed algorithms that retrieve bottom reflectance signals by reducing depth effects and minimizing impacts of turbidity.The water-depth correction algorithms were developed and improved by empirically separating the energy absorbed and scattered by varying depths of water using

DOI: 01.IJIT.3.1. 1138

data collected through a series of controlled experiments [16], [17], [18], [19]. The series of algorithms successfully removed the overlying water effects and restored the reflectance obtained from laboratory-measured submerged vegetation [17]. The results demonstrated that the NIR signals originating from seagrass-dominated sea floors were significantly restored when applied to airborne hyperspectral data [16], [18]. Thus far, the absorption and scattering values that were used in the algorithms were derived from clear water, which do not suitably mimic natural waters. In this paper, the algorithm was improved to correct both water depth and water turbidity that interfere with remote sensing of seagrass beds and embedded in a user-friendly Graphical User Interface (GUI).

III. Matetials and Methods

Laboratory experiments were conducted in a dark room in order to include water turbidity as a factor in the model, following the methods by [17], [18], and [19]. Known amounts of fine sand were measured and added to an experimental water tank (170 litres) to simulate different levels of water turbidity. Prior to being added, the fine sand was thoroughly cleaned with tap water, oven-dried, and combusted to remove any organic matter. After the sand was added to the tank, the water was consistently stirred to keep the sediment suspended and then was left undisturbed for 5 minutes before the turbidity was measured using a LaMotte 2020e Turbidimeter unit (LaMotte Company, Chestertown, Maryland). Upwelling radiance from the tank water was scanned at varying depths (5 cm intervals from 0 to 60 cm) using an Ocean Optics USB 2000+ spectroradiometer with a fiber optic sensor (Ocean Optic Inc., Dunedin, FL). The same measurements were made over waters with varying turbidity values (0, 5, 10, 15, 20 Nephalometric Turbidity Unit-NTU). Reflectance (%) values were calculated only between 500 and 840 nm in order to reduce noise in the signals below or above the wavelength regions.

IV. Results and Discussion

A. Water Correction Algorithm for Turbid Water

Water absorption and volumetric reflectance (%) values were calculated at the varying water depths (0-60 cm) and turbidity levels (0-20 NTU) using the algorithm by [18]. As expected, water absorption increases with water depth and turbidity. A nonlinear function was constructed to fit samples through the regression analysis: measured reflectance (%) = $(ax^3 + bx^2 + cx + 1)y^d$, where a, b, c, and d are the parameters obtained through regression analysis, x denotes water turbidity value in NTU, and y represents water depth in centimeters. The regression analysis was then applied to all bands. For example, the regression equation at 675 nm was $(0.013x^3 + 0.486x^2 + 5.357x + 1)y^{-0.672}$. When the standard deviation of the regression analysis for water absorption at the bands was calculated, most values were less than 1.4 and less than 1.0 at the NIR bands. The following equation was developed to calculate water absorption (%):

$$Abs = p_1 \tanh(y/q_1)(a_1x^3 + b_1x^2 + c_1x + 1)y^{d1}. \quad (1)$$

A similar procedure was used to develop the following equation for volumetric reflectance (%):

$$Vol = (p_2 \exp(q_2y) + r)(a_2x^3 + b_2x^2 + c_2x + 1)y^{d2}. \quad (2)$$

All parameters, a_1, b_1, c_1, d_1, p_1, q_1, a_2, b_2, c_2, d_2, p_2, q_2, and r, were obtained through regression analysis and varied with bands. The absorption and volumetric reflectance from (1) and (2) were then applied to the algorithms proposed by [17] and [18] to perform water correction.

B. Building Graphical User Interface

A Graphical User Interface (GUI) was built using Interactive Data Language (IDL) Version 7.1 in order to provide the prospective users with a user friendly interface that can be applied to perform water correction of hyperspectral images containing information on shallow water bodies. The benefit of using IDL is that the GUI can be easily incorporated in the IDL-based image processing software, ENVI (Environment for Visualizing Images), and expand the ENVI functions. The water correction GUI contains two sub-interfaces: (1) Image specification; and (2) Correction performance.

The hyperspectral image data used in this paper were obtained using AISA Eagle Hyperspectral Sensor (Galileo Inc., Finland) over an area of Mission-Aransas National Estuarine Research Reserve in Texas. The image contains shallow (< 2 m) bays areas where seagrass is abundant. Prior to the water correction using the GUI, the image was preprocessed to remove atmospheric effects using FLAASH. All pixel values were converted to percent reflectance.

C. Image Specification

In the first window of the GUI (Fig. 1), users are required to put information about the configuration of the raw image. The "X-Dim" denotes the number of columns in the image, the "Y-Dim" denotes the number of rows, and "Bands" denotes the total number of bands (Fig. 1). The image dimensions and band information can be obtained from the header file of the image. After clicking the "Read Wavelength from File" button (Fig. 1), Users will be prompted by a pop-up window to select the header information file.The header information file is a textual file that contains two lines. The first line contains the dimensions of the image. For example, the values 98, 116 and 63 in the first line indicate that the image has 98 rows, 116 columns, and 63 bands. The second line shows all the bands in nanometers (nm). Users are required to construct their own header information files accordingly. After reading the header file information, the second GUI page can be accessed by clicking "continue" or otherwise users can exit the GUI by clicking the "cancel" button (Fig. 1).

D. Correction Performance using the GUI

The pop-up window for the second GUI interface is shown in Fig. 2. After clicking the "Input Raw Image File" button, users can select the input image file to be corrected. The input image can either be in a textual or binary format. Users can assign the name of the output image by clicking "Output

DOI: 01.IJIT.3.1.1138

Corrected File". Then, users must confirm the formats of input file accordingly.The optional field, "DN to Reflectance Factor" (Fig. 2), is used to input a scaling factor that can convert Digital Numbers (DN) into % reflectance values unless the DN values already represent % reflectance. Users are required to determine this value based on the source of the raw image data. The water depth and turbidity values are then selected using two slide buttons. At this time, the correction algorithm can only be applied to images that have homogenous water depth conditions. Users should click the "Run Correction Algorithm" button for processing to begin (Fig. 2). When the message "——Finish One Image Correction ————" is printed in the command terminal, the correction procedure is completed.

Fig. 1. Series of pop-up windows in image specification stage of water correction GUI: GUI of image dimension description (upper panel); file information input window (lower panel)

The GUI interface provides three ways to examine the efficiency of the water correction algorithm by analyzing the corrected image. One is to draw a spectral profile of a specific region/pixel. Users can choose the region/pixel location of the image by setting the pixel values under "Area Location (x1, y1) to (x2, y2)" (Fig. 2). After determining the location, users can click the "Draw Profile" button in Fig. 2. The contrast between the raw and the corrected image at this area/pixel will be displayed likewise in Fig. 3. Fig. 3 shows comparison of the spectral profiles between the uncorrected raw image pixel and the pixel after a water correction. The spectral reflectance in the NIR region noticeably increased after the water correction (Fig. 3), which is an important outcome of this algorithm because the model restored the NIR reflectance from the seagrass pixels. The NIR information provides critical vegetation information including presence/abundance, and health of seagrass beds, benthic algae, and algae on coral reefs (Fig. 3). However, the exponentially increasing reflectance at the wavelengths longer than 820 nm indicates that the water correction model coefficients over-estimated water attenuation factors at these wavelengths.

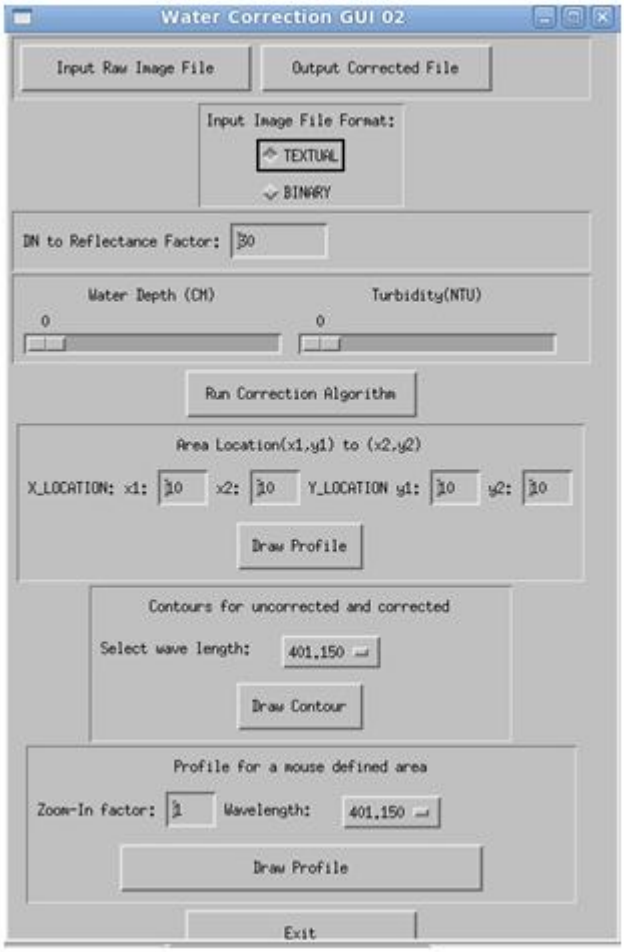

Fig. 2. Main pop-up windows in correction performance stage of water correction GUI.

Another way to evaluate the water correction results is to compare the reflectance values of the original and the corrected images at a user-defined wavelength. Users first select a band by clicking the "select wavelength" button in Fig. 2, and then click the "Draw Contour" button. A new pop-up window will appear as shown in Fig. 4. The visual image comparison between the original and the water-effect corrected images will give the users a more intuitive understanding about the image processing results. The contrast between the bare sediment and seagrass patches was enhanced after the correction (Fig. 4).Alternatively, users can select a subset area of the image for water correction by using a cursor (Fig. 2). Because an image size could be too small or too large to select easily, a zoom-in factor can be inputted by users. Users must then determine the wavelength for viewing. A pop-up window will display as shown in Fig. 5

DOI: 01.IJIT.3.1. 1138

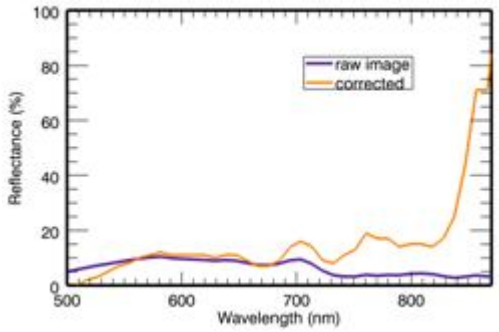

Fig. 3. Comparison of spectral profiles of a selected pixel in an AISA image, taken over a seagrass bed, before and after the water correction

(right panel). Users can select a rectangle by dragging the left button of the mouse over an area of interest. Subsequently, the button "Draw Profile" in Fig. 2 is pressed to display the contrast in the reflectance of the original and water correction images. Users can quit the correction process and exit the GUI by clicking the "Exit" button in Fig. 2.

The water-corrected pixel values at the red and the NIR wavelengths (i.e. 670 nm and 740 nm, respectively) can further be used to calculate conventional vegetation indices such as normalized difference vegetation index (NDVI = $(R_{NIR} - R_R)/(R_{NIR} + R_R)$), where R_{NIR} is the reflectance at a NIR band and R_R is the reflectance at a Red band. The index uses the difference in the reflectance between the two bands to distinguish photosynthesizing plants from other substrates. Due to the strong absorption in the NIR region, the NDVI values calculated from uncorrected digital numbers (DN) are smaller than 0 even for the pixels containing thick seagrass beds (Fig. 6, upper panel). After the water correction, the NDVI effectively distinguishes seagrass pixels (pixels with higher NDVI values) from those over bare sediments (Fig. 6, lower panel).

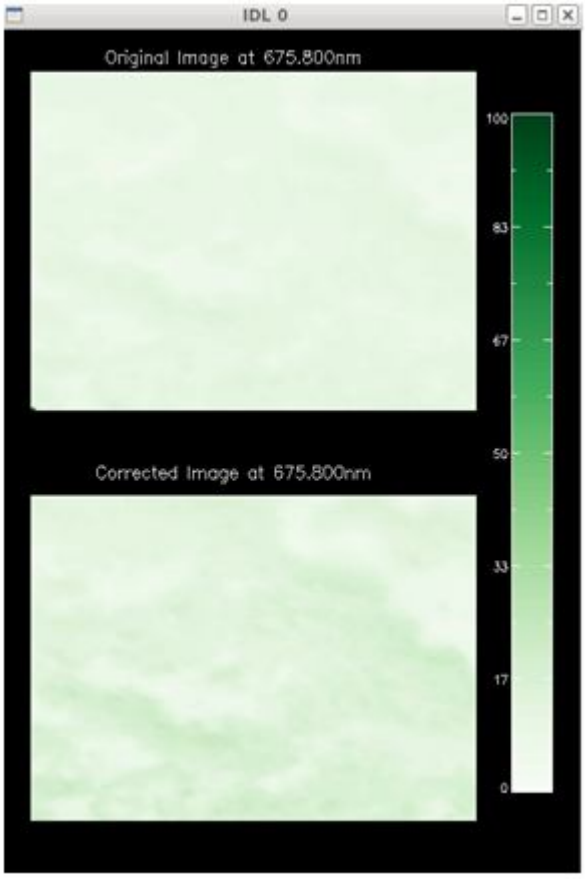

Fig. 4. Example of original (above) and water correction (below) images at a selected wavelength of 675.8 nm

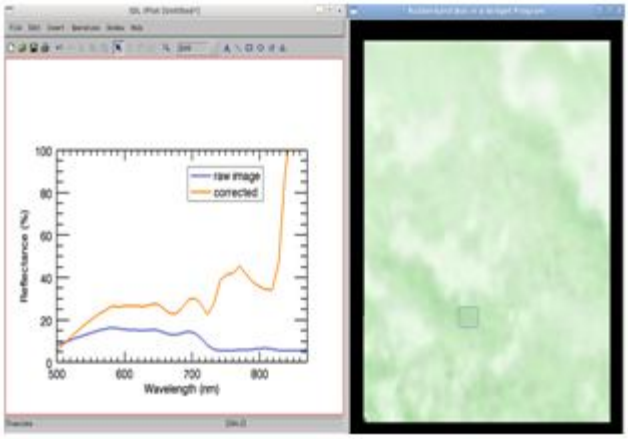

Fig. 5. Example of mouse-selected area window and corresponding area averaged reflectance profiles before and after correction

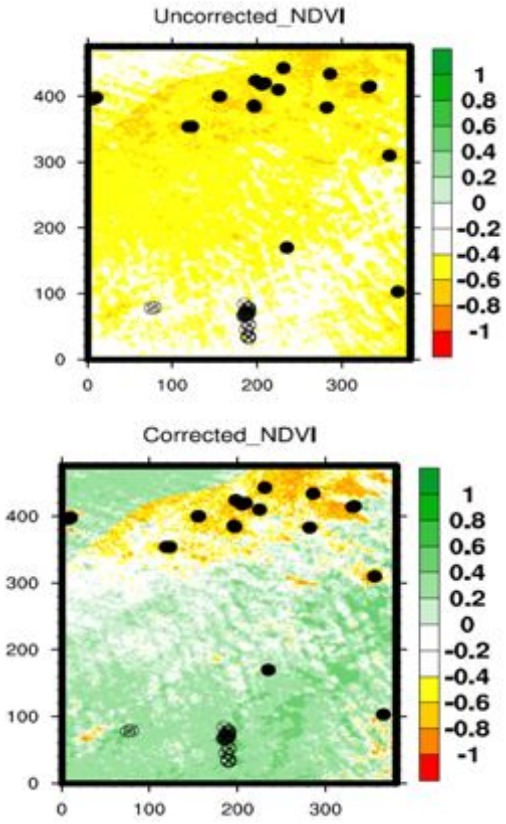

Fig. 6. An image subset of NDVI (normalized difference vegetation index) values calculated from the original % reflectance values (above panel) and from the water-corrected values. The average NDVI values calculated at the selected pixels (represented by the circles: the closed circles represent selected seagrass pixels; and the open circles are bare sediment pixels) were -0.19 before the correction and 0.28 after the correction.

DOI: 01.IJIT.3.1.1138

Conclusions

A Graphical User Interface (GUI) was built using Interactive Data Language (IDL) Version 7.1 in order to provide the prospective users with a novel, user friendly interface that can be applied to perform water correction of hyperspectral images containing shallow water bodies. The significance and innovation of this GUI is the user-friendly application of the improved water correction algorithm and module in shallow coastal benthic mapping using spaceborne/ airborne hyperspectral data. The application will be best used in mapping of submerged aquatic vegetation since the algorithm restores reflectance in the NIR region. The GUI for the model application can be added to menus in currently available commercial image processing software (i.e. ENVI®). Occasionally, underflow may occur as users perform the water correction. This probably occurs because: (1) the water depth and/or water turbidity selection is not suitable for the image being processed; or (2) the value of the "DN to Reflectance Factor" is not appropriate. As mentioned earlier, the exponentially increasing reflectance in Fig. 5 at the wavelengths longer than 820 nm is erroneous indicating the water correction model coefficients over estimated water attenuation factors at these wavelengths.

Acknowledgment

This research is supported by the grants from the National Geospatial-Intelligence Agency (Grant Nos. HM1582-07-1-2005 and HM1582-08-1-0049) and the National Oceanic and Atmospheric Administration–Environmental Cooperative Sciences Center (NOAA–ECSC). The image data were collected and pre-processed by the Center for Advanced Land Management Information Technologies (CALMIT), University of Nebraska-Lincoln, and distributed through NOAA-ECSC. We sincerely thank Dr. John Schalles of Creighton University for sharing the water quality data and the Jackson State University students, Philemon Kirui and Marvin Washington, who assisted with the field and experimental data collection. The authors also thank Dr. Duanjun Lu and Dao Lu for their contribution to the data analyses and GUI development.

References

[1] S.M. Adler-Golden, A. Berk, L.S. Bernstein, S.C. Richtsmeier, P.K. Acharya, M.W. Matthew, G. P.Anderson, C.L. Allred, L.S. Jeong, and J.H. Chetwynd, "FLAASH, a MODTRAN4 AtmosphericCorrection Package for Hyperspectral Data Retrievals and Simulations," 1998 AVIRIS Geoscience Workshop, Jet Propulsion Laboratory, Pasadena, California, 1998

[2] H. Holden and E. LeDrew, "Effects of the Water Column on Hyperspectral Reflectance of Submerged Coral Reef Features," B. Mar. Sci., vol. 69, pp. 685-699, 2001.

[3] H. Holden and E. LeDrew, "Measuring and Modeling Water Column Effects on Hyperspectral Reflectance in a Coral Reef Environment," Remote Sens. Environ., vol. 81, pp. 300-308, 2002.

[4] G. Ciraolo, E. Cox, G. La Loggia, and A. Maltese, "TheClassification of Submerged Vegetation Using Hyperspectral MIVIS Data," AGp, vol. 49, pp. 287-294, 2006.

[5] D.R. Mishra, S. Narumalani, D. Rundquist, and M.P. Lawson "Benthic Habitat Mapping in Tropical Marine Environments Using QuickBird Imagery," Photogramm. Eng. Rem. S., vol. 72, pp. 1037-1048, 2006.

[6] V.E. Brando, J.M. Anstee, M. Wettle, A.G. Dekker, S.R. Phinn, C. and Roelfsema, "A Physics Based Retrieval and Quality Assessment of Bathymetry from Suboptimal Hyperspectral Data," Remote Sens. Environ., vol. 113, pp. 755-770, 2009.

[7] E. M. Louchard, R. P. Reid, F. C. Stephens, C. O. Davis, R. A. Leathers, and T. V. Downes, "Optical remote sensing of benthic habitats and bathymetry in coastal environments at Lee Stocking Island, Bahamas: A comparative spectral classification approach," Limnol. Oceanogr., vol. 48, pp. 511–521, 2003.

[8] Z. P. Lee, K. L. Carder, C. D. Mobley, R. G. Steward, and J. F. Patch, "Hyperspectral remote sensing for shallow waters: II. deriving bottom depths and water properties by optimization," Appl. Opt., vol. 38. pp. 3831-3843, 1999.

[9] C.M. Hu, Z.Q. Chen, T.D. Clayton, P. Swarzenski, J.C. Brock, and F.E. Muller-Karger, "Assessment of estuarine water-quality indicators using MODIS medium-resolution bands: Initial results from Tampa Bay, FL," Remote Sens. Environ., vol. 93, pp. 423–441, 2004.

[10] D. R. Lyzenga, "Passive remote sensing techniques for mapping water depth and bottom features" Appl. Opt., vol. 17, pp. 379–383, 1978.

[11] D. R. Lyzenga, "Remote sensing of bottom reflectance and water attenuation parameters in shallow water using aircraft and Landsat data," International Journal of Remote Sensing, vol. 2, pp. 71–82, 1981.

[12] H. M. Dierssen, R. C. Zimmerman, R. A. Leathers, T. V. Downes, and C. O. Davis, "Ocean color remote sensing of seagrass and bathymetry in the Bahamas Banks by high resolution airborne imagery," Limnol. Oceanogr., vol. 48, pp. 444-455, 2003.

[13] J. Maeder, S. Narumalani, D.C. Rundquist, R.L. Perk, J. Schalles, K, Hutchins, K., and J. Keck, "Classifying and Mapping General Coral-reef Structure using Ikonos Data," Photogramm. Eng. Rem. S., vol. 68, pp. 1297-1305, 2002.

[14] V. Pasqualini, C. Pergent-Martini, G. Pergent, M. Agreil, G. Skoufas, L. Sourbes, and A. Tsirika, "Use of SPOT 5 for Mapping Seagrasses: An Application to Posidonia oceanic," Remote Sens. Environ., vol. 94, pp. 39-45, 2005.

[15] T. Kutser, E. Vahtmae, and J. Praks, "A sun glint correction method for hyperspectral imagery containing areas with non-negligible water leaving NIR signal," Remote Sens. Environ., vol. 113, pp. 2267-2274, 2009

[16] H.J. Cho, D. Lu, and M. Washington, "Water Correction Algorithm Application for Underwater Vegetation Signal Improvement," In Proceedings of the 2009 MS Water Resource Conference, pp 114-117. Mississippi, 2009.

[17] H.J. Cho, and D. Lu, "A Water-depth Correction Algorithm for Submerged Vegetation Spectra," Remote Sens. Lett. vol. 1, pp. 29 – 35, 2010.

[18] D. Lu, and H.J. Cho, "An Improved Water-depth Correction Algorithm for Seagrass Mapping Using Hyperspectral Data," Remote Sens. Lett. vol. 2, pp. 91 – 97, 2011

[19] M. Washington, P. Kirui, H.J. Cho, and C. Wafo-soh, "Data-driven Correction for Light Attenuation in Shallow Waters," Remote Sens. Lett. vol. 3, pp. 335-342, 2012.

DOI: 01.IJIT.3.1. 1138